

The Hanbury Brown-Twiss effect in a pulsed atom laser

A. G. Manning, S. S. Hodgman, R. G. Dall,
M. T. Johnsson, and A. G. Truscott*

*ARC Centre of Excellence for Quantum-Atom Optics
and Research School of Physics and Engineering,
Australian National University, Canberra, ACT 0200, Australia*

[*andrew.truscott@anu.edu.au](mailto:andrew.truscott@anu.edu.au)

Abstract: We have used the Hanbury Brown-Twiss effect to directly compare the density correlations of a pulsed atom laser and a pulsed ultracold thermal source of metastable helium. It was found that the isotropic RF outcoupling of atoms from a Bose-Einstein condensate does not result in decoherence, while the ‘bunching’ typical of incoherent sources was observed for thermal atoms. This new method significantly increases data acquisition rates compared to previous measurements, and also permits future novel experiments which may allow us to probe processes such as the birth and death of a condensate by monitoring correlation effects.

© 2010 Optical Society of America

OCIS codes: (020.0020) Atomic and molecular physics; (020.1335) Atom optics; (020.1475) Bose-Einstein condensates.

References and links

1. R. Hanbury Brown and R. Q. Twiss, “Correlation between photons in two coherent beams of light,” *Nature* **177**, 27–29 (1956).
2. M. Yasuda and F. Shimizu, “Observation of Two-Atom Correlation of an Ultracold Neon Atomic Beam,” *Phys. Rev. Lett.* **77**, 3090-3093 (1996).
3. K. G. H. Baldwin, “Metastable helium: atom optics with nano-grenades,” *Cont. Phys.* **46**, 105–120 (2005).
4. O. Jagutzki, V. Mergel, K. Ullmann-Pfleger, L. Spielberger, U. Meyer, R. Drner, and H. Schmidt-Böcking, “Fast Position and Time Resolved Read-Out of Micro-Channelplates with Delay-Line Technique for Single Particle and Photon Detection,” *Proc. SPIE* **3438**, 322 (1998).
5. M. Schellekens, R. Hoppeler, A. Perrin, J. Viana Gomes, D. Boiron, A. Aspect and C. I. Westbrook, “Hanbury Brown Twiss Effect for Ultracold Quantum Gases,” *Science* **310**, 648–651 (2005).
6. T. Jelten, J. M. McNamara, W. Hogervorst, W. Vassen, V. Krachmalnicoff, M. Schellekens, A. Perrin, H. Chang, D. Boiron, A. Aspect and C. I. Westbrook, “Comparison of the Hanbury Brown-Twiss effect for bosons and fermions,” *Nature* **445**, 402–405 (2007).
7. A. Öttl, S. Ritter, and M. Köhl and T. Esslinger, “Correlations and Counting Statistics of an Atom Laser,” *Phys. Rev. Lett.* **95**, 090404 (2005).
8. R. G. Dall and A. G. Truscott, “Bose-Einstein condensation of metastable helium in a bi-planar quadrupole Ioffe configuration trap,” *Opt. Commun.* **207**, 255–261 (2006).
9. M.-O. Mewes, M. R. Andrews, D. M. Kurn, D. S. Durfee, C. G. Townsend, and W. Ketterle, “Output Coupler for Bose-Einstein Condensed Atoms,” *Phys. Rev. Lett.* **78**, 582-585 (1997).
10. M. Naraschewski and R. J. Glauber, “Spatial coherence and density correlations of trapped Bose gases,” *Phys. Rev. A* **59**, 4595–4607 (1999).
11. J. Viana Gomes, A. Perrin, M. Schellekens, D. Boiron, C. I. Westbrook and M. Besley, “Theory for a Hanbury Brown Twiss experiment with a ballistically expanding cloud of cold atoms,” *Phys. Rev. A* **74**, 053607 (2006).
12. R. G. Dall, L. J. Byron, A. G. Truscott, G. R. Dennis, M. T. Johnsson, M. Jeppesen and J. J. Hope, “Observation of transverse interference fringes on an atom laser beam,” *Opt. Express* **15**, 17673–17680 (2007).
13. M. Schellekens, “L’Effet Hanbury Brown et Twiss pour les Atomes Froids,” PhD. Thesis (2007).
14. I. Bloch, T. Hänsch and T. Esslinger, “Measurement of the spatial coherence of a trapped Bose gas at the phase transition,” *Nature* **403**, 166–169 (2000).

1. Introduction

Correlation measurements are a powerful way of exploring fundamental quantum mechanical phenomena which arise purely from the quantum statistics of particles. These effects can be quantified with correlation functions, the order of which distinguishes the type of correlation. The most familiar correlation function is that of the first order, which describes amplitude interferometry, and is related to the fringe visibility in a double slit experiment. However, while the first order correlation function is highly sensitive to phase fluctuations, the second order correlation function provides a simple way of differentiating between different types of source. These sources can be primarily classified as either thermal (incoherent) fermions, thermal bosons, and coherent bosons, which will have different density (or intensity) correlations as evident from their second order correlation functions.

The appeal of second order correlations was first realised in a stellar interferometry experiment by Hanbury Brown and Twiss, who attempted to measure the angular width of stars [1], which are incoherent sources of bosons. Thermal bosons were found to arrive at the detector in ‘bunches’, where the likelihood of measuring a photon a very short time after the previous one increases as the path length difference between the interferometer arms was reduced. On the other hand, no correlations exist in a second order-coherent source such as an optical laser operating well above threshold. Although initial experiments were conducted in the 1950s with light, the field of atom optics has progressed over the last two decades to the point where ultracold neutral atom clouds suitable for the demonstration of this so-called Hanbury Brown-Twiss (HBT) effect can be created [2]. By cooling the atoms to ultracold temperatures, their de Broglie wavelength becomes sufficiently large for intensity correlations to be measured with current experimental techniques.

Previous experiments measuring the HBT effect in neutral atoms can be categorised by the method of outcoupling and detecting the atoms. One technique is a sudden magnetic trap switch-off, which drops ultracold clouds onto a detector capable of measuring single atoms. In this case, metastable helium (He^*) is an ideal species to use as its ~ 20 eV of internal energy [3] permits the use of a microchannel plate and delay-line detector, which offers unique single atom detection capabilities with three-dimensional information [4]. This method was used to demonstrate the ‘bunching’ of thermal atoms and lack of correlations in the atomic equivalent of a laser, the Bose-Einstein condensate (BEC), in $^4\text{He}^*$ [5]. Similarly, ‘anti-bunching’ was observed in a thermal source of fermionic $^3\text{He}^*$ [6].

Another approach has been to continuously outcouple trapped atoms using narrowband radiation [7]. As ^{87}Rb was used in this case, a high finesse cavity was implemented to measure temporal information for single atoms. While a direct comparison of an atom laser and continuous thermal source was not possible, bunching was observed in a pseudothermal beam.

Vast amounts of data are required to ensure robust statistics for correlation measurements, however data acquisition rates in previous experiments using He^* [5,6] and Rb [7] were limited by either low atomic flux or detector saturation. The stability of our BiQUIC magnetic trap [8] permits the use of a pulsed atomic source, circumventing the saturation of the detector which increases our data acquisition rate by an order of magnitude.

In addition, we are able to investigate whether any decoherence of the condensate occurs when atoms are outcoupled with broadband radiation. Such radiation interacts with the atom cloud isotropically and gives a representative sample of the entire cloud. The dynamics of the outputcoupling process, however, are significantly different to those induced by a sudden switch off of the magnetic trapping potential. First, the outcoupled pulse interacts with the still-trapped dense condensate, thereby evolving under stronger atom-atom interactions [9]. Second, when atoms are coupled out the mean-field repulsion inside the condensate is reduced which can lead to collective oscillations and possible multi-mode behaviour of the cloud [9]. These

oscillations lead to fluctuations in the condensate density, and are thus possible sources for loss of pulse coherence. Third, the outcoupled pulse is transferred into the $m_f = 0$ state resulting in Penning processes which produce charged particles and low energy neutral helium atoms. Fourth, by outcoupling multiple pulses (up to 30) in the same realisation of the experiment we probe the long term (up to a second) stability of the second order correlation function of the system. Hence, our method can be thought of as a minimally destructive real time probe of the coherence properties of the ultracold atom cloud, enabling new experiments that probe the evolution of temporal correlations of the entire cloud to be performed, allowing the formation of the BEC to be studied in detail.

2. Background

2.1. Second Order Correlation Function

The Hanbury Brown-Twiss effect can be understood by considering the second order correlation function $g^{(2)}(\mathbf{r}_1, \mathbf{r}_2; t_1, t_2)$, which is the joint probability of simultaneously measuring two particles at positions and times (\mathbf{r}_1, t_1) and (\mathbf{r}_2, t_2) [10]. It is defined in Eq. (1) as

$$g^{(2)}(\mathbf{r}_1, \mathbf{r}_2; t_1, t_2) = \frac{G^{(2)}(\mathbf{r}_1, \mathbf{r}_2; t_1, t_2)}{\sqrt{G^{(2)}(\mathbf{r}_1, \mathbf{r}_1; t_1, t_1)G^{(2)}(\mathbf{r}_2, \mathbf{r}_2; t_2, t_2)}}, \quad (1)$$

$$G^{(2)}(\mathbf{r}_1, \mathbf{r}_2; t_1, t_2) = \langle \hat{O}^\dagger(\mathbf{r}_1, t_1) \hat{O}^\dagger(\mathbf{r}_2, t_2) \hat{O}(\mathbf{r}_2, t_2) \hat{O}(\mathbf{r}_1, t_1) \rangle, \quad (\text{for pure states}) \quad (2)$$

where \hat{O} in Eq. (2) is the operator representing measurement. For example, if we use stationary pure boson modes where measurement is performed with the annihilation operator \hat{a} for an interferometer with path time difference τ , then (suppressing spatial coordinates) we get Eq. (3)

$$g^{(2)}(\tau) = \frac{\langle \hat{a}^\dagger(0) \hat{a}^\dagger(\tau) \hat{a}(\tau) \hat{a}(0) \rangle}{\langle \hat{a}^\dagger(0) \hat{a}(0) \rangle^2}. \quad (3)$$

By taking $\tau = 0$, and given that $[\hat{a}, \hat{a}^\dagger] = 1$ yields Eq. (4)

$$\begin{aligned} g^{(2)}(0) &= \frac{\langle \hat{a}^\dagger \hat{a} \rangle^2 + \langle (\hat{a}^\dagger \hat{a})^2 \rangle - \langle \hat{a}^\dagger \hat{a} \rangle^2 - \langle \hat{a}^\dagger \hat{a} \rangle}{\langle \hat{a}^\dagger \hat{a} \rangle^2}, \\ &= 1 + \frac{\sigma_n^2 - \langle \hat{a}^\dagger \hat{a} \rangle}{\langle \hat{a}^\dagger \hat{a} \rangle^2}, \end{aligned} \quad (4)$$

where the variance in expected number is $\sigma_n^2 = \langle (\hat{a}^\dagger \hat{a})^2 \rangle - \langle \hat{a}^\dagger \hat{a} \rangle^2$. The difference between thermal and coherent sources can be understood given the dependence on this variance. For a thermal source with expected number $\langle \hat{a}^\dagger \hat{a} \rangle = n$, $\sigma_n^2 = n^2 + n$ leads to $g^{(2)}(0) = 2$ which is the ‘bunching’ of incoherent bosons where a pair of atoms arriving simultaneously is twice as likely as would occur if no correlations existed. However, for second order-coherent state $|\alpha\rangle$ with $\langle \hat{a}^\dagger \hat{a} \rangle = |\alpha|^2$, $\sigma_n^2 = |\alpha|^2$ and thus $g^{(2)}(0) = 1$, and in fact $g^{(2)}(\tau) = 1 \forall \tau$ which means that the arrival times of coherent bosons on the detector follows an uncorrelated Poissonian distribution at all times.

In general, $g^{(2)}(\tau) \rightarrow 1$ monotonically as τ becomes large, as correlations ‘wash out’ at large temporal (or equivalently spatial) separations. The time over which correlations persist is an important consideration for designing experiments, and the use of massive particles adds complexity compared to correlation measurements with light. Detailed analysis [11] has shown that for a thermal atom cloud dropped under gravity in the z direction from a magnetic trap will have a correlation time $t^{(\text{cor})} = l_z / v_z$, where the correlation length at the detector is $l_z = \hbar t / (m s_z)$

for drop time t , velocity at detector v_z , and atom mass m of a cloud of size s_z in the magnetic trap. We can use $s_z = [kT/(m\omega_z^2)]^{1/2}$ for atoms at temperature T in a harmonic trap of with frequency ω_z in the z direction.

Although the above equations hold for a single cloud dropped from a trap, the situation for a continuously outcoupled thermal beam is different. In the z direction, the correlation time will instead be $t^{(\text{cor})} = \hbar/\Delta E$ for energy spread ΔE [11].

2.2. Motivation for pulsed beam

The use of a continuously outcoupled thermal beam results in a significant reduction in the correlation time for helium. If we outcouple isotropically such that $\Delta E = mv\Delta v$ for $\Delta v = [kT/m]^{1/2}$, the correlation time would be of order 100 ns for our experiment at 850 nK, compared to ~ 120 μs for dropped clouds. Continuous outcoupling thus requires a lengthy data acquisition process, as the limited flux measurable on our detector leads to a low likelihood of a pair of atoms being detected within the short correlation time. If we instead outcouple in a spatially selective manner to reduce the energy spread, then ΔE at the detector would be greater for He* than for other species such as rubidium [7] due to the ellipsoid shape of its outcoupling surface [12].

We cannot increase the data acquisition rate by simply dropping larger clouds onto the detector, due to saturation which occurs for pulses of $\sim 10^5$ atoms. However, we trap $\sim 10^6$ atoms and apply a series of Fourier broadened RF pulses to emulate the repeated dropping of small clouds, which significantly improves the duty cycle and collection efficiency as we do not discard many atoms. In contrast, the peak flux measurable with a cavity is typically ~ 1 kHz [7], approximately three orders of magnitude less than a delay-line detector. Our method samples the cloud isotropically, rather than outcoupling from a localised region, which gives a better representation of the entire cloud. Also, by only outcoupling a small portion of the atoms at once, we cause minimal perturbation to the cloud. Finally, this method allows $g^{(2)}$ of an atom laser to be directly compared to that of an RF outcoupled thermal source for the first time, by measuring the two under identical conditions.

3. Experimental Setup and Method

3.1. Apparatus

The basic experimental apparatus has been described previously [8]. A recent addition, however, was the installation of a Roentdek DLD80 delay-line detection system located 800 mm below the magnetic trap, which provides high-resolution temporal and spatial measurements of single metastable helium atoms (see Fig. 1).

The specifications of the delay-line detector are a spatial resolution found to be consistent with manufacturers claim of ~ 100 μm , a maximum flux of 1 MHz, and a dead time of 20 ns. Our resolution was estimated from an image produced by atoms passing through a calibration test mask situated 10 mm above the detection system. This is in contrast to the apparatus used in a previous similar experiment, which operated at a flux of ~ 700 kHz and a resolution of ~ 250 μm [13], so our new detection system should in principle yield superior results.

3.2. Method

Ultracold clouds of He* were created using the methods outlined in [8]. The radial trapping frequency for the magnetic trap was $2\pi \times 500$ Hz, while the axial frequency was $2\pi \times 50$ Hz. Atoms were then released from the trap at 29 ms intervals using 20 μs pulses of RF radiation, which spin-flips them to a field-insensitive state. Given that the pulses had a larger Fourier width than both the chemical potential of the condensate ~ 8 kHz and the thermal width of the non-degenerate cloud ~ 30 kHz, the radiation interacted with the atoms in the cloud uniformly

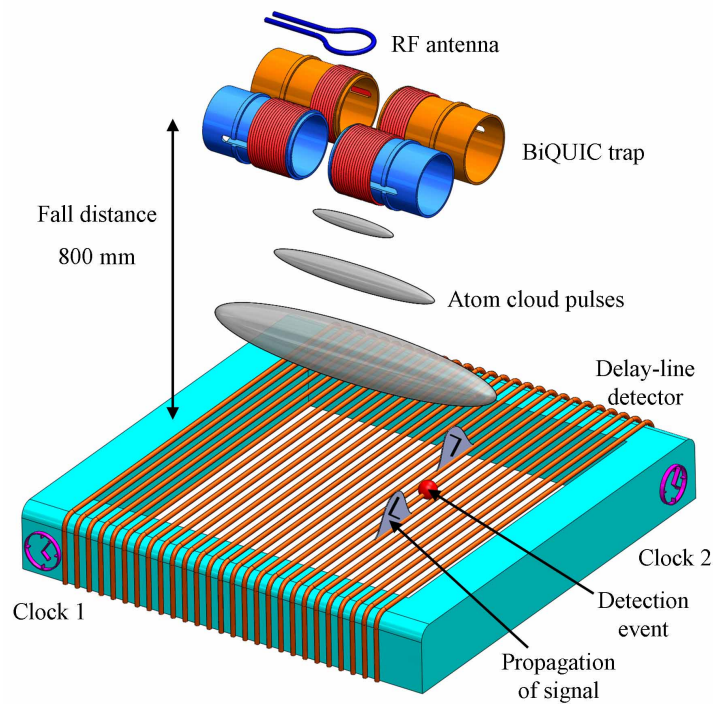


Fig. 1. Atoms are outcoupled in pulses from the BiQUIC trap using RF radiation, and fall under gravity onto the detection system below. A micro-channel plate (not shown) allows single atoms to be measured on a delay-line detector, which causes a signal pulse to propagate in both directions along two helical delay-line wires for a 2D spatial image (only one wire shown). The time taken for the signal to reach the ends of each wire is measured, from which the arrival time and position can be calculated [4].

over a wide range of energies, or equivalently all spatial positions in the trap, giving a good representative sample of the cloud.

The atoms were then dropped ~ 800 mm under gravity onto a micro-channel plate and delay-line detector (see Fig. 1), which recorded the arrival time and position of each atom detected. The large drop distance is desirable to increase the transverse correlation length of the thermal clouds which reduces the washing out of the signal due to finite detector resolution. The second order correlation function $g^{(2)}(\tau)$ was calculated for two separate experimental runs, one for thermal atoms slightly above the condensation temperature, and the other for a pulsed atom laser. To achieve this, for each detection event we found the time difference τ between this and subsequent atoms landing no more than $700 \mu\text{m}$ away. These time differences were used to create a histogram with $20 \mu\text{s}$ bins, which gave the unnormalised correlation function $G^{(2)}(\tau)$. This was then normalised by the autocorrelated bulk intensity profile to find $g^{(2)}(\tau)$.

4. Results

4.1. Intensity profile

The temporal intensity profile of atoms detected, averaged for 10 experimental cycles of atoms above the condensation temperature, is shown in Fig. 2. The $20 \mu\text{s}$ RF bursts resulted in each pulse of atoms arriving at the detector in a ~ 20 ms window. The final, high flux peak was the

atoms remaining in the trap after the 30 RF pulses being dropped when the magnetic trap was switched off.

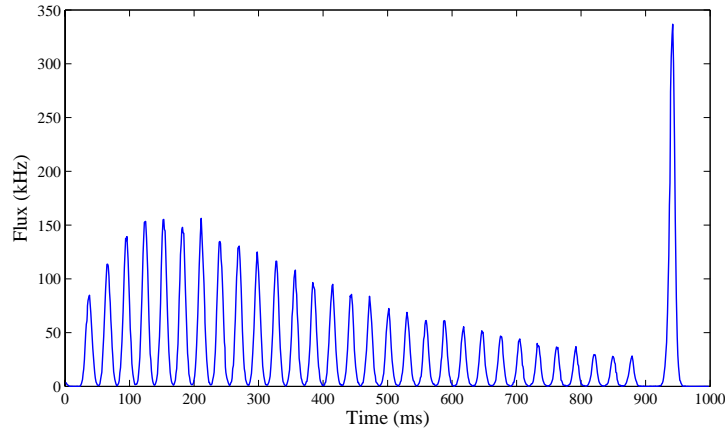


Fig. 2. Intensity of thermal atoms arriving at detector binned in 1 ms increments. The time-of-flight profile for the atom laser is similar, albeit for narrower pulses with a lower temperature. The power of the RF outcoupling is increased during the experimental cycle to make the relative intensity of the atomic pulses more uniform

The temperature of each thermal pulse was 850 ± 100 nK. This temperature spread slightly changed the bunching amplitude ($g^{(2)} - 1$) of the correlation function measured. Condensates were identified easily given the shape of the spatial intensity profile measured on the detector, and as such we tuned the cooling process to finish either side of the condensation temperature. Given the stability of our trap, condensates or thermal clouds were created in a controlled and repeatable manner. The pulsed atom laser was created by outcoupling atoms from a BEC in the same way.

4.2. Correlation function

The correlation plot for thermal atoms (Fig. 3) was calculated from 1700 experimental cycles resulting in $\sim 10^5$ correlated pairs per $20 \mu\text{s}$ time bin. The correlation time of the thermal atoms was found to be $102 \mu\text{s}$, given by the width of a Gaussian fit, where the theoretical estimate is $120 \pm 20 \mu\text{s}$. Given we typically form a condensate at around 600 nK, the correlation time cannot be increased significantly under these experimental conditions. The bunching amplitude in the plot of 0.024 is lower than the ideal value of 1, due to factors such as the finite resolution of the detector and the spatial binning of detections into discs of diameter $700 \mu\text{m}$, the latter being chosen to maximise the signal to noise ratio. While smaller bins lead to a superior bunching amplitude as the correlated pair detections are less likely to become washed out by pairs with large separations, more data needs to be acquired as the number of pair detections per bin will decrease, leading to larger relative shot noise.

A simulation which accounts for our spatial binning regime and detector resolution was performed to determine the anticipated bunching amplitude. The detector resolution is included as an effect which increases the average observed distance between pairs of atoms separated by a distance comparable to the resolution. The bunching amplitude for a pair of atoms at this adjusted separation distance was then computed using the model developed by Viana Gomes et al. [11], and then averaged for a collection of pair detections generated uniformly within a disc of diameter $700 \mu\text{m}$. While this simple model was somewhat dependent on assumptions

such as the influence of detector resolution, a bunching amplitude of $\sim 4\%$ was expected. The discrepancy between our calculated and measured correlation amplitude and time is due to effects including imperfections in the normalisation of the experimental correlation function.

Although our signal to noise ratio is currently limited by statistical error, by binning at a resolution limit of $100 \mu\text{m}$ we may be able to increase our bunching amplitude by an order of magnitude, which is not possible with a detector of significantly poorer resolution, nor is it an appealing notion if acquiring data at a much slower rate. Nonetheless, a correlation function with similar signal to noise as previous experiments [5] was achieved, verifying the validity of our method.

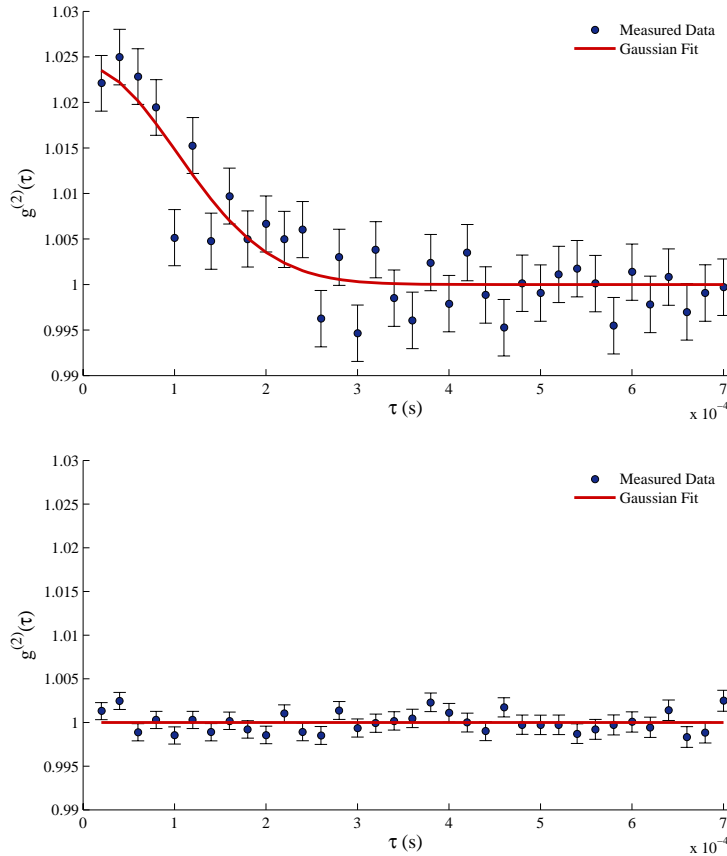


Fig. 3. Plot of second order correlation function $g^{(2)}(\tau)$ for thermal atoms at 850 nK (top) and for a pulsed atom laser (bottom). The error bars shown are shot noise.

The correlation function for the pulsed atom laser (Fig. 3), produced from 1700 experimental cycles with $10^5 - 10^6$ correlated pairs per $20 \mu\text{s}$ time bin, was also fitted to a Gaussian function in the same manner as for the thermal clouds. However, the best fit was for a bunching amplitude of zero, meaning that no bunching was observed in the pulsed atom laser. In general, the observation of bunching of thermal atoms is difficult, as the temperature must be low enough to ensure that the correlation time is sufficiently large, and the detector resolution must be good enough to prevent $g^{(2)}(\tau)$ from washing out to unity. However, given that we observed bunching in thermal bosons, yet no bunching for a pulsed atom laser under identical conditions,

we can conclusively see that the coherence of the atom laser has not been compromised by the outcoupling process.

5. Conclusion

We have directly compared the second order correlations of a pulsed atom laser and pulsed thermal source, and found this to be the same as for dropping single clouds [5]. This demonstrates that the RF outcoupling process does not perturb the second order coherence of the atoms. Considering the tendency of helium to fountain upwards and thus have a large spread in momentum as it is outcoupled [12], as well as losses due to Penning ionisation [3], one would suspect that helium is a species at high risk of decoherence upon outcoupling. Therefore, our results indicate that any other species should retain coherence when outcoupled in this way. Also, this measurement was carried out an order of magnitude faster than previous experiments [13], meaning data with a similar signal to noise ratio to previous results can now be acquired in a day.

Given our ability to outcouple pulses of atoms in a controllable way, especially considering that they are in a field-insensitive state, this new method allows future experiments to be performed which could lead to a more thorough investigation of how the correlation function changes with time across a phase transition. Although this has been performed with first order correlation functions [14], this would be the first time that the second order coherence of an atom cloud crossing the condensation threshold could be probed using unambiguous density correlations.

Acknowledgements

This work is supported by the Australian Research Council Centre of Excellence for Quantum-Atom Optics.